Motions in a Bose condensate: VII. Boundary-layer separation

2000 J. Phys. A: Math. Gen. 33 4025

(http://iopscience.iop.org/0305-4470/33/22/307)

J. Phys. A: Math. Gen. **33** (2000) 4025–4038. Printed in the UK PII: S0305-4470(00)11351-4

Motions in a Bose condensate: VII. Boundary-layer separation

Natalia G Berloff and Paul H Roberts

Department of Mathematics, University of California, Los Angeles, CA, 90095-1555, USA

E-mail: nberloff@math.ucla.edu and roberts@math.ucla.edu

Received 26 January 1999, in final form 17 April 2000

Abstract. The Bose condensate model is used to analyse the superfluid flow around an ion (modelled as a solid sphere) and to elucidate the mechanism of vortex ring emission from the sphere that occurs if its velocity exceeds a critical value. An asymptotic expansion is developed for the steady subcritical flow, using the ratio of the healing length to the radius of the sphere as a small parameter. This expansion allows for the compressibility of the condensate, and converges well enough for the critical ion velocity to be calculated accurately. The flow for supercritical ion velocities is computed numerically. Particular attention is paid to the question of why the vortex rings are emitted at a preferred location on the sphere's surface.

1. Introduction

This is the seventh in a series of papers devoted to the Bose condensate as applied to superfluid helium and especially superfluid vortices (see Roberts and Grant 1971, Grant 1973, Grant and Roberts 1974, Jones and Roberts 1982, Jones *et al* 1986, Berloff and Roberts 1999).

Vortex nucleation by an impurity such as the positive ion $^4He_2^+$ moving in superfluid helium at low temperature has been studied experimentally and theoretically (see, e.g., Donnelly 1991), and has uncovered some interesting physics. The flow around an ion that is moving with a sufficiently small velocity, v, is well represented by one of the classical solutions of fluid mechanics, namely the flow of an inviscid incompressible fluid around a sphere. In this solution, the maximum flow velocity, $\boldsymbol{u}$, relative to the sphere is $3v/2$, and occurs on the equator of the sphere (defined with respect to the direction of motion of the sphere as the polar axis). Above some critical velocity, v_c, the ideal superflow around the ion breaks down, leading to the creation of a vortex ring (Rayfield and Reif 1964). The critical velocity can be roughly estimated by arguing that the vortex will be nucleated from the point where the relative velocity of the ion and superfluid is greatest (the equator), and will occur when that velocity reaches the Landau critical velocity, v_L. If, using the incompressible model, we estimate the relative velocity as $3v/2$, we find that $v_c \approx 2v_L/3$, in rough agreement with experiment (see table 8.2 of Donnelly (1991)). Because $2v_L/3$ is only about 15% of the speed of sound, c, it appears that the incompressible model should perform reasonably well, and that an allowance for the compressibility of the superfluid is not a high priority. This was the basis of the original paper by Strayer *et al* (1971) and the later developments of Muirhead *et al* (1984), who created a theory of vortex nucleation that allowed them to calculate v_c, the form of the potential barrier that must be overcome for the creation of vortices both as encircling rings and vortex loops, and the nucleation rate. These calculations were carried out for a smooth rigid sphere moving through an ideal incompressible fluid.

0305-4470/00/224025+14$30.00

The Bose condensate offers a different insight into the nucleation process. The condensate is a weakly interacting Bose gas that, in the Hartree approximation, is governed by an equation for the single-particle wavefunction $\psi(\boldsymbol{x}, t)$ that was first derived by Ginzburg and Pitaevskii (1958) and Gross (1963); see (1) below. Using this equation, Grant and Roberts (1974) studied the negative ion (the electron bubble) and a positive ion, modelling the latter as a spherical, infinite potential barrier, on the surface of which ψ vanishes. Their solutions were derived by expansion in v/c, so that their leading-order flow is incompressible. They did not observe vortex nucleation.

As a model of superfluidity, the condensate suffers from the defect that its dispersion relation does not possess a roton minimum, so that $v_L = c$. To observe vortex nucleation therefore, Grant and Roberts (1974) would have had to develop expansions appropriate for a compressible flow in which $\boldsymbol{u} = \mathcal{O}(c)$, which they did not do (although we do so in section 3 below). It is possible to make the condensate model more realistic by replacing the δ-function interaction potential between atoms, on which it is based, by a non-local potential. This restores the roton minimum and a realistic v_L but only at the expense of considerable complexity (see Berloff 1999). As for the most recent research on this topic (e.g. Frisch *et al* 1992, Winiecki *et al* 1999), we shall employ the condensate model in its original form.

An important scale defined by the condensate model is the 'healing length', a, defined in (10) below. This determines the radius of a vortex core and the thickness of the 'healing layer' that forms at a potential barrier (such as the ion surface in our model). The radius, b, of the ion is large compared with a, and asymptotic solutions for $\epsilon \equiv a/b \to 0$ become relevant; see section 3. Such a solution has two parts, an interior or 'boundary-layer' structure that matches smoothly to an exterior or 'mainstream' flow. In the mainstream, quantum effects are negligible at leading order, and the condensate becomes effectively a compressible inviscid fluid obeying the simple equation of state, $p \propto \rho^2$, where p is pressure and ρ is density (see (8) below).

There is some similarity between the flow of the condensate past the ion and the motion of a viscous fluid past a sphere at large Reynolds numbers, the healing layer being the counterpart of the viscous boundary layer. There are, however, important differences. At subcritical velocities, the flow of the condensate is symmetric fore and aft of the direction of motion, and the sphere experiences no drag. In contrast, the viscous boundary layer separates from the sphere, so evading D'Alembert's paradox, destroying the fore and aft symmetry, and therefore bringing about a drag on the sphere. Moreover, when $v > v_c$, shocks form at or near the sphere, but shocks are disallowed in the condensate since they represent a violation of the Landau criterion and a breakdown of superfluidity. When $v > v_c$, the condensate evades shocks through a different mode of boundary-layer separation. The sphere sheds circular vortex rings that move more slowly than the sphere and form a vortex street that trails behind it, maintained by vortices that the sphere sheds. As the velocity of the ion increases such a shedding becomes more and more irregular. Each ring is born at one particular latitude within the healing layer on the sphere. As it breaks away into the mainstream, it at first contributes a flow that depresses the mainstream velocity on the sphere below the critical value. As it moves further downstream, however, its influence on the surface flow diminishes. The surface flow increases until it again reaches criticality, when a new ring is nucleated and the whole sequence is repeated. The vortex street trailing behind the ion creates drag on the ion that decreases as the nearest vortex moves downstream, but which is refreshed when a new vortex is born.

Frisch *et al* (1992) and Winiecki *et al* (1999) have solved the condensate equation for flow past a circular cylinder, and have confirmed the main features of the scenario just described. In this paper, we present analogous solutions for a more realistic geometry. By employing a convergent series expansion suitable for $\boldsymbol{u} = \mathcal{O}(c)$, we determine v_c for $\epsilon = 0$ more

accurately than before. We confirm this value through numerical integrations at finite ϵ, while simultaneously obtaining indications of how v_c depends on ϵ. (We should observe here that the criterion $v = c$ for criticality applies only for $\epsilon = 0$. The velocity in a healing layer can exceed c without implying nucleation. For example, $\boldsymbol{u}$ in a vortex core actually becomes infinite, according to the condensate model!) We also show how and why the vortex ring detaches, not from the equator of the ion, but from a latitude downstream of it. We find how this latitude depends on v.

Since Bose–Einstein condensation of dilute gases in traps was observed experimentally in 1995 (for a review of the experimental and theoretical results, see Dalfovo *et al* 1999) attempts were made to produce and detect quantized vortices in such gases. The existence of quantized vortices would establish an important connection between Bose condensation and superfluidity. As the Bose–Einstein condensates in the experiments are formed as small spheres of atoms, held in place by magnetic traps the motion of these spheres should cause the formation of quantized vortices. Therefore, our theory could be tested experimentally and is potentially useful in interpreting experimental results.

2. The condensate equation

According to the Bose condensate model, $\psi(\boldsymbol{x}, \boldsymbol{t})$ in an assembly of N bosons of mass M, is governed by the nonlinear Schrödinger equation

$$\mathrm{i}\hbar\frac{\partial\psi}{\partial t} = -\frac{\hbar^2}{2M}\nabla^2\psi - \psi\left(E + \tfrac{1}{2}Mv^2 - V_0|\psi|^2\right) \tag{1}$$

where V_0 is the strength of the δ-function interaction potential between the bosons and E is the single-particle energy in the laboratory frame, where the ion moves with velocity v in the positive z-direction through a fluid at rest at infinity. Equation (1) is written for the ion reference frame, in which the fluid at infinity is moving with velocity v in the negative z-direction and the ion is at rest. Thus we require that

$$\psi \to \psi_\infty \exp\left[-\frac{\mathrm{i}Mvz}{\hbar}\right] \qquad \text{for} \quad \boldsymbol{x} \to \infty \tag{2}$$

where $\psi_\infty = (E/V_0)^{1/2}$.

We ignore the effect of the electric charge on the ion, and model it as a sphere of radius b that is an infinite potential barrier to the condensate, so that

$$\psi = 0 \qquad \text{at} \quad r = b. \tag{3}$$

Here we have introduced a spherical coordinate system (r, θ, ϕ), with its origin at the centre O of the ion, and with $\theta = 0$ as the z-axis. The wavefunction is required to obey the normalization condition on the total number of bosons $N = \int |\psi|^2 \,\mathrm{d}V$. The mass density and flux are

$$\rho = M\psi\psi^* \qquad \boldsymbol{j} = \frac{\hbar}{2\mathrm{i}}(\psi^*\boldsymbol{\nabla}\psi - \psi\boldsymbol{\nabla}\psi^*). \tag{4}$$

Equation (1) can be written in hydrodynamic form through the Madelung transformation,

$$\psi = R\mathrm{e}^{\mathrm{i}S} \tag{5}$$

so that

$$\rho = MR^2 \qquad \boldsymbol{j} = \rho\boldsymbol{u} = \rho\nabla\phi \qquad \phi = (\hbar/M)S. \tag{6}$$

The real and imaginary parts of (1) then yield a continuity equation

$$\frac{\partial \rho}{\partial t} + \nabla \cdot (\rho \boldsymbol{u}) = 0 \tag{7}$$

and an integrated form of the momentum equation

$$\frac{\partial \phi}{\partial t} + \frac{1}{2}u^2 - \frac{1}{2}v^2 + c^2\left(\frac{\rho}{\rho_\infty} - 1\right) - \frac{\hbar^2}{2M^2}\frac{\nabla^2 \rho^{1/2}}{\rho^{1/2}} = 0 \tag{8}$$

the last term of which is often called the 'quantum pressure', although dimensionally it is a chemical potential. Also appearing in (8) are the density at infinity ρ_∞ and the speed of sound c:

$$\rho_\infty = M\psi_\infty^2 \qquad c^2 = E/M. \tag{9}$$

We also define the healing length, a, as

$$a = \frac{\hbar}{(2ME)^{1/2}}. \tag{10}$$

The boundary conditions (2) and (3) give

$$\rho \to \rho_\infty \qquad \boldsymbol{u} \to -v\mathbf{1}_z \qquad \text{for} \quad \boldsymbol{x} \to \infty \tag{11}$$

$$\rho = 0 \qquad j_r = 0 \qquad \text{on} \quad r = b \tag{12}$$

where $\mathbf{1}_q$ denotes the unit vector in the direction of increasing coordinate q. There is no requirement that $u_r = 0$ on $r = b$; indeed, the problem would be overdetermined if we applied that condition.

3. Asymptotic expansion for velocities up to criticality

In this section, we develop the asymptotic expansion of solutions for small $\epsilon \equiv a/b$. We suppose that the speed of the ion is comparable with the speed of sound c, so that the effects of compressibility cannot be ignored. The appropriate non-dimensionalization of (1) is

$$\boldsymbol{x} \to b\boldsymbol{x} \qquad t \to \big(abM/\hbar\big)t \qquad v \to \big(\hbar/aM\big)U \qquad \psi \to \psi_\infty \psi. \tag{13}$$

Subcritical flow is steady in the ion reference frame, and the Madelung equations are therefore

$$\epsilon^2\nabla^2 R - R(\nabla S)^2 = (R^2 - 1 - U^2)R \tag{14}$$

$$R\nabla^2 S + 2\nabla R \cdot \nabla S = 0. \tag{15}$$

The quantum pressure term, $\epsilon^2\nabla^2 R$ is negligibly small in the far field but is of major importance in the boundary layer, for which we set $r = 1 + \epsilon\xi$, and expand R and S as

$$R(\xi, \theta) = \widehat{R}_0(\xi, \theta) + \epsilon\widehat{R}_1(\xi, \theta) + \epsilon^2\widehat{R}_2(\xi, \theta) + \cdots \tag{16}$$

$$S(\xi, \theta) = \widehat{S}_0(\xi, \theta) + \epsilon\widehat{S}_1(\xi, \theta) + \epsilon^2\widehat{S}_2(\xi, \theta) + \cdots. \tag{17}$$

Equations (14) and (15) give $\partial\widehat{S}_0/\partial\xi = \partial\widehat{S}_1/\partial\xi = 0$, so that

$$\widehat{S}_0 = \widehat{S}_0(\theta) \qquad \widehat{S}_1 = \widehat{S}_1(\theta) \tag{18}$$

where $\widehat{S}_0(\theta)$ and $\widehat{S}_1(\theta)$ are to be determined by matching to u_θ on $r = 1$ in the mainstream. After we substitute the $\widehat{S}_0$ into (14), it becomes to leading order

$$\frac{\partial^2\widehat{R}_0}{\partial\xi^2} - \widehat{R}_0^3 + \widehat{R}_0\big[1 + U^2 - (\widehat{S}_0'(\theta))^2\big] = 0 \tag{19}$$

so that

$$\widehat{R}_0 = g(\theta)\tanh(g(\theta)\xi/\sqrt{2}) \tag{20}$$

where

$$g(\theta) = \sqrt{\left[1 + U^2 - (\widehat{S}_0'(\theta))^2\right]}. \tag{21}$$

The equation governing $\widehat{S}_2$ is

$$\frac{\partial}{\partial\xi}\left(\widehat{R}_0^2\frac{\partial\widehat{S}_2}{\partial\xi}\right) = -\frac{1}{\sin\theta}\frac{\partial}{\partial\theta}\left[\widehat{R}_0^2\sin\theta\frac{\mathrm{d}\widehat{S}_0}{\mathrm{d}\theta}\right]. \tag{22}$$

This gives $\widehat{S}_2$ as

$$\widehat{S}_2 = -\frac{1}{\sin\theta}\frac{\partial}{\partial\theta}\left(h(\xi,\theta)\sin\theta\frac{\mathrm{d}\widehat{S}_0}{\mathrm{d}\theta}\right) + \zeta_2(\theta) \tag{23}$$

where

$$h(\xi,\theta) = \int_0^\xi \frac{\mathrm{d}\xi'}{\widehat{R}_0^2(\xi',\theta)}\int_0^{\xi'}\widehat{R}_0^2(\xi'',\theta)\,\mathrm{d}\xi'' = \frac{1}{2}\xi^2 - \frac{\sqrt{2}\xi}{g(\theta)}\coth\left(\frac{g(\theta)\xi}{\sqrt{2}}\right) \tag{24}$$

and $\zeta_2(\theta)$ is a function of integration that can be determined by matching to the mainstream.

To leading order, the mainstream flow is the classical inviscid compressible flow past a sphere, and is governed by

$$R^2 = 1 + U^2 - (\nabla S)^2 \tag{25}$$

$$R^2\nabla^2 S + \nabla R^2\cdot\nabla S = 0. \tag{26}$$

We substitute the first equation of this system into the second one to obtain an equation for S alone. We then expand S as in (17) and then expand $S_0, S_1, \ldots$ in powers of U, for example,

$$S_0(r,\theta) = U S_{11}(r)P_1(\cos\theta) + U^3(S_{31}(r)P_1(\cos\theta) + S_{33}(r)P_3(\cos\theta)) + \cdots. \tag{27}$$

For U close to the speed of sound, $c = 1/\sqrt{2}$, we do not expect (27) to converge fast enough to be useful, but the critical U which we are trying to determine is approximately $2c/3$ and for such values of U the expansion (27) converges fast enough. We expand S to the U^{11} term in order to obtain an estimate for the critical velocity of nucleation, U_c, accurate to 1%. The first few equations for the mainstream are

$$\frac{\mathrm{d}^2S_{11}}{\mathrm{d}r^2} + \frac{2}{r}\frac{\mathrm{d}S_{11}}{\mathrm{d}r} - \frac{2S_{11}}{r^2} = 0 \tag{28}$$

$$\begin{aligned}\frac{\mathrm{d}^2S_{31}}{\mathrm{d}r^2} + \frac{2}{r}\frac{\mathrm{d}S_{31}}{\mathrm{d}r} - \frac{2S_{31}}{r^2} &= \frac{9}{5}\left(\frac{\mathrm{d}S_{11}}{\mathrm{d}r}\right)^2\frac{\mathrm{d}^2S_{11}}{\mathrm{d}r^2} + \frac{2S_{11}^2}{r^2}\frac{\mathrm{d}^2S_{11}}{\mathrm{d}r^2}\\ &\quad + \frac{6}{5r}\left(\frac{\mathrm{d}S_{11}}{\mathrm{d}r}\right)^3 + \frac{2S_{11}}{5r^2}\left(\frac{\mathrm{d}S_{11}}{\mathrm{d}r}\right)^2 - \frac{8S_{11}^3}{5r^4}\end{aligned} \tag{29}$$

$$\begin{aligned}\frac{\mathrm{d}^2S_{33}}{\mathrm{d}r^2} + \frac{2}{r}\frac{\mathrm{d}S_{33}}{\mathrm{d}r} - \frac{12S_{33}}{r^2} &= \frac{6}{5}\left(\frac{\mathrm{d}S_{11}}{\mathrm{d}r}\right)^2\frac{\mathrm{d}^2S_{11}}{\mathrm{d}r^2} - \frac{2S_1^2}{5r^2}\frac{\mathrm{d}^2S_{11}}{\mathrm{d}r^2}\\ &\quad + \frac{4}{5r}\left(\frac{\mathrm{d}S_{11}}{\mathrm{d}r}\right)^3 - \frac{12S_1}{5r^2}\left(\frac{\mathrm{d}S_{11}}{\mathrm{d}r}\right)^2 + \frac{8S_{11}^3}{5r^4}.\end{aligned} \tag{30}$$

Solving these, we obtain

$$S_{11} = -r - \frac{1}{2r^2} \qquad S_{33} = -\frac{3}{88r^8} + \frac{3}{5r^5} + \frac{3}{5r^2} + \frac{C_1}{r^4} \qquad S_{31} = -\frac{1}{12r^8} + \frac{2}{5r^5} + \frac{C_2}{r^2}. \tag{31}$$

To carry out the asymptotic matching, we substitute $r = 1 + \epsilon\xi$ in the expressions for $S_{11}, S_{31}, S_{33}, \ldots$, expand the solution in powers of ϵ, and match it to the boundary-layer solution. The first few terms of the resulting mainstream solution are

$$\begin{aligned} S_0(r,\theta) = &-\frac{3U\cos\theta}{2r^2} + U^3\left(\left[-\frac{1}{12r^8} + \frac{2}{5r^5} - \frac{2}{3r^2}\right]\cos\theta \right. \\ &\left. +\left[-\frac{3}{88r^8} + \frac{3}{5r^5} - \frac{54}{55r^4} + \frac{3}{5r^2}\right]P_3(\cos\theta)\right) \\ &+U^5\left(\left[-\frac{1901}{18\,480r^{14}} + \frac{1739}{2310r^{11}} - \frac{5589}{21\,175r^{10}}\right.\right. \\ &\left.-\frac{1766}{1155r^8} + \frac{972}{1925r^7} + \frac{776}{525r^5} - \frac{1470\,911}{1016\,400r^2}\right]\cos\theta \\ &+\left[-\frac{179}{2244r^{14}} + \frac{7256}{8085r^{11}} - \frac{2274}{3575r^{10}} - \frac{523}{220r^8}\right. \\ &\left.+\frac{624}{275r^7} + \frac{152}{75r^5} - \frac{72\,781\,521}{23\,823\,800r^4} + \frac{106}{75r^2}\right]P_3(\cos\theta) \\ &+\left[-\frac{1945}{140\,448r^{14}} + \frac{2291}{9240r^{11}} - \frac{87}{385r^{10}} - \frac{295}{182r^8}\right. \\ &\left.\left.+\frac{240}{77r^7} - \frac{51\,393}{434\,720r^6} - \frac{68}{21r^5} + \frac{24}{11r^4} - \frac{10}{21r^2}\right]P_5(\cos\theta)\right) + \cdots. \end{aligned} \tag{32}$$

From this we can determine the first function of (18):

$$\begin{aligned} S_0(\theta) = &-\tfrac{3}{2}U\cos\theta - \tfrac{7}{20}U^3\cos\theta + \tfrac{81}{440}U^3P_3(\cos\theta) \\ &+U^5\left[-\tfrac{14\,693}{24\,200}\cos\theta + \tfrac{1560\,249}{3403\,400}P_3(\cos\theta) - \tfrac{31\,857}{217\,360}P_5(\cos\theta)\right] + \cdots. \end{aligned} \tag{33}$$

The maximum flow velocity is attained on the equator and is, to leading order in ϵ,

$$\begin{aligned} u_{0\theta}(1, \tfrac{1}{2}\pi) = &\,3U/2 + 0.626\,136U^3 + 1.569\,61U^5 \\ &+5.181\,61U^7 + 19.9015U^9 + 84.2325U^{11} + \cdots \end{aligned} \tag{34}$$

where here we have included terms up to order U^{11}. The flow (34) reaches the speed of sound if the far-field velocity U is approximately 0.415. An idea of the accuracy of this value of U_c is obtained by comparing it with the final term of (34), which for $U_c = 0.415$ is 0.005. The result also agrees very well with the numerical calculations of section 5 for small ϵ. By comparing 0.41 with $2c/3 \approx 0.471$, we gain an impression of the importance of compressibility in determining U_c in the condensate model.

The $\mathcal{O}(\epsilon)$ contribution to the mainstream solution satisfies the following equations:

$$R_0R_1 = -\nabla S_0 \cdot \nabla S_1 \tag{35}$$

$$2R_0R_1\nabla^2 S_0 + R_0^2\nabla^2 S_1 + 2\nabla\big(R_0R_1\big)\cdot\nabla S_0 + \nabla R_0^2 \cdot \nabla S_1 = 0. \tag{36}$$

We substitute the first equation of this system into the second one to obtain the equation for S_1 and expand S_1 as in (27) to the U^5 term. The first few terms of the resulting mainstream

solution are

$$S_1(r,\theta) = U\frac{D_1}{r^2}\cos\theta + U^3\left(\left[\frac{D_1}{2r^8} - \frac{8D_1}{5r^5} + \frac{D_2}{r^2}\right]\cos\theta \right.$$
$$\left. + \left[\frac{9D_1}{44r^8} - \frac{12D_1}{5r^5} - \frac{6D_1}{5r^2} + \frac{D_3}{r^4}\right]P_3(\cos\theta)\right) + \cdots. \tag{37}$$

The unknown constants are found by matching the boundary-layer solution (23) to (37). We substitute $r = 1 + \epsilon\xi$ in (37), expand the solution in powers of ϵ, and note that the last term in (24) is $\mathcal{O}(\xi)$ for $\xi \to \infty$. We expand the corresponding term of $\widehat{S}_2$ for large ξ in powers of U and in the Legendre polynomials, and set the coefficients of the resulting expansion equal to the corresponding coefficients at the order ϵ in the expansion of (37). This defines the constants in (37) as

$$D_1 = -\frac{3}{\sqrt{2}} \qquad D_2 = -\frac{79}{10\sqrt{2}} \qquad D_3 = -\frac{783}{110\sqrt{2}}. \tag{38}$$

On the equator of the sphere the ϵ term of the expansion of u_θ is

$$u_{1\theta}(1, \tfrac{1}{2}\pi) = 2.121\,32U + 3.165\,91U^3 + 11.582\,55U^5 + \cdots. \tag{39}$$

The interesting question is whether the S_1 term increases or decreases U_c. This raises the philosophical point touched on in section 1: is the Landau criterion precise when we go beyond the leading term in the $\boldsymbol{u}$ expansion of the mainstream by including the ϵ term associated with the quantum pressure? We are encouraged to believe it is; because of the upward curvature of the dispersion curve associated with the condensate model, the speed of long-wavelength sound plausibly sets the stability limit for all disturbances. We therefore now set $u_\theta(1, \frac{1}{2}\pi) = c$, where u_θ includes (34) and (39). For $\epsilon = 0.1$ the resulting U_c is approximately 0.36, which is less than the value ($U_c \approx 0.39$) suggested by the numerical calculations of section 5, whereas $u_{0\theta}$ alone gave a value greater than 0.39, i.e. the zeroth and first approximations bracket the correct answer for U_c at finite ϵ.

4. Asymptotic expansion for the cylinder

In considering the shedding of line vortices from a moving cylinder, Frisch *et al* (1992) gave an argument for the critical velocity that we shall now test through an expansion of the same type as that of the preceding section. Instead of (27), we now use a Fourier expansion in θ, which is one of the cylindrical coordinates (r, θ, z), with $\theta = 0$ parallel to $\boldsymbol{U}$:

$$S_0 = US_{11}(r)\cos\theta + U^3(S_{31}(r)\cos\theta + S_{33}(r)\cos 3\theta) + \cdots. \tag{40}$$

The mainstream solution is found to be

$$S_0(r,\theta) = -U\left(r + \frac{1}{r}\right)\cos\theta + U^3\left[\left(-\frac{1}{6r^2} + \frac{1}{r^3} - \frac{13}{6r}\right)\cos\theta + \left(-\frac{1}{r^3} + \frac{1}{2r}\right)\cos 3\theta\right]$$
$$+U^5\left[\left(-\frac{7}{30r^9} + \frac{3}{2r^7} - \frac{43}{12r^5} + \frac{35}{6r^3} - \frac{479}{60r}\right)\cos\theta\right.$$
$$+\left(-\frac{1}{36r^9} + \frac{4}{15r^7} - \frac{3}{2r^5} + \frac{43}{30r^3} + \frac{19}{12r}\right)\cos 3\theta$$
$$\left.+\left(\frac{7}{20r^5} - \frac{1}{2r^3} - \frac{1}{4r}\right)\cos 5\theta\right] + \cdots. \tag{41}$$

The boundary-layer function corresponding to (18) is

$$\widehat{S}_0(\theta) = -2U\cos\theta + U^3\left(-\tfrac{4}{3}\cos\theta + \tfrac{1}{3}\cos 3\theta\right) + U^5\left(-\tfrac{67}{15}\cos\theta + \tfrac{79}{45}\cos 3\theta - \tfrac{2}{5}\cos 5\theta\right) + U^7\left[-\tfrac{251}{12}\cos\theta + \tfrac{203\,933}{18\,900}\cos 3\theta - \tfrac{80\,113}{18\,900}\cos 5\theta + \tfrac{11}{14}\cos 7\theta\right] + \mathrm{O}(U^9). \tag{42}$$

The maximum flow velocity, which occurs on the cylinder equator, is

$$u_{0\theta}(1, \tfrac{1}{2}\pi) = 2U + 7U^3/3 + 176U^5/15 + 79.9809U^7 + 552.181U^9 + 4471.18U^{11} + \cdots. \tag{43}$$

This reaches the velocity of sound for $U = U_c \approx 0.30$. (To illustrate the convergence of (43), we note that the U^{11} term is only 0.0066 for $U = 0.30$.)

According to Frisch *et al* (1992), criticality is reached when, in our non-dimensional units, the velocity exceeds $\rho/2$ anywhere in the mainstream. In applying their criterion, they assumed that the maximum velocity can be well approximated by its value, $2U$, in an incompressible flow, and it followed that at criticality $U_c \approx 0.302$, which is in agreement with their numerical integrations. A similar critical velocity was obtained by Winiecki *et al* (1999). Although this result is close to the value of the critical velocity we derived above, equation (43) shows that the assumption of incompressibility does not provide a good estimate of the maximum velocity. In fact, when (43) is used, the argument of Frisch *et al* (1992) gives a critical velocity of $U_c \approx 0.26$, which is very different from the results of the numerical integration.

5. Numerical calculations

In this section we present some results from numerical calculations for the axisymmetric flow around the sphere and the nucleation of vortex rings from it. We used a different non-dimensionalization of (1):

$$\boldsymbol{x} \to a\boldsymbol{x} \qquad t \to (a^2M/\hbar)t \qquad v \to (\hbar/aM)U \qquad \psi \to \left(\psi_\infty \mathrm{e}^{-\mathrm{i}Uz}\right)\psi \tag{44}$$

the last of which removes the uniform flow $-v\mathbf{1}_z$ everywhere, so that

$$\psi \to 1 \qquad \text{as} \quad r \to \infty. \tag{45}$$

Equation (1) becomes

$$-2\mathrm{i}\frac{\partial\psi}{\partial t} + 2\mathrm{i}U\frac{\partial\psi}{\partial z} = \nabla^2\psi + \psi(1 - |\psi|^2) \tag{46}$$

the solution to which must satisfy (45) and

$$\psi = 0 \qquad \text{on} \quad r = b/a. \tag{47}$$

We employed a finite-difference scheme to solve (46) in the axisymmetric case in which ψ depends only on r and θ, and in which therefore

$$-2\mathrm{i}\frac{\partial\psi}{\partial t} + 2\mathrm{i}U\cos\theta\,\psi_r - 2\mathrm{i}U\frac{\sin\theta}{r}\psi_\theta = \frac{\partial^2\psi}{\partial r^2} + \frac{2}{r}\frac{\partial\psi}{\partial r} + \frac{\cot\theta}{r^2}\frac{\partial\psi}{\partial\theta} + \frac{1}{r^2}\frac{\partial^2\psi}{\partial\theta^2} + \psi(1 - |\psi|^2). \tag{48}$$

The integration box was chosen as $[b/a, r_1] \times [0, \pi]$. One of the main considerations in choosing the integration scheme was that outgoing sound waves should escape from the integration box. We used the Raymond–Kuo (1984) radiation boundary condition on $r = r_1$. In time stepping the leap-frog scheme was implemented with a backward Euler step every 100 steps to prevent the even–odd instability. In space we used a fourth-order finite-difference scheme together with a second-order scheme close to the boundary $r = r_1$. The code was

tested against the asymptotic solutions of section 3. The initial condition for velocities slightly larger than U_c was chosen as $\psi = \tanh(\xi/\sqrt{2})$. The numerical scheme does not conserve energy but the dissipation of energy is very small. When reflective boundary conditions were used instead of radiative ones, the energy loss due to the dissipative character of the scheme did not exceed $10^{-4}\%$ per 1000 time steps.

Our numerical work strongly suggests that the value of U_c (≈ 0.415) obtained in section 3 for $\epsilon = 0$ is correct. We also found that U_c decreases with decreasing ϵ, in agreement with the analysis of section 3.

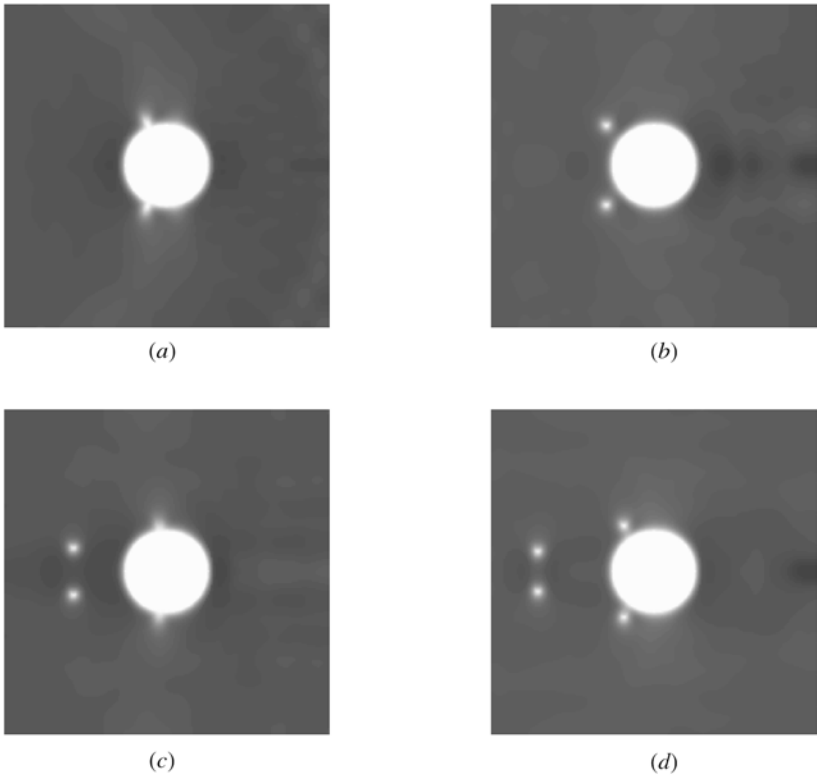

Figure 1. The density plot in a cross section of the solution of (48) for the flow around a sphere of radius 10 moving to the right with velocity 0.42 at (*a*) $t = 68$, (*b*) $t = 124$, (*c*) $t = 212$ and (*d*) $t = 268$. Vortex rings appear as white circles close to the sphere and gradually fall astern of the ion.

Figure 1 shows the formation of the ring from a sphere of radius 10 moving with supercritical velocity $U = 0.42$. After the ion emits a vortex ring, the flow associated with the ring at first makes the total mainstream velocity subcritical everywhere. The self-induced velocity of the ring is less than the velocity of the ion, so that the ring gradually falls astern of the ion and the total fluid velocity builds up until it again reaches criticality on the surface of the ion. The vortex ring emission follows the same scenario as that observed by Frisch *et al* (1992) for vortex pair nucleation from a cylinder (see section 1). What came as a surprise is that, although the maximum velocity of the compressible flow is always attained on the equator of the sphere, the vortex ring nucleates from the sphere downstream of the equator, at $\theta_c > \frac{1}{2}\pi$. This is clearly seen in figure 1(*a*), which shows the birth of the first vortex after the motion of the ion has been initiated. The first nucleation seems to be the result of an instability of the

critical flow (obtained from section 3, as described above). The second nucleation is influenced by the presence of the first ring (see figure 1(*b*)). It therefore takes place at a different location on the ion surface, as is readily seen in figures 1(*c*) and (*d*).

It is difficult to extend the theory of section 3 to cover the time-dependent supercritical state that arises when vortices are nucleated. It is, however, comparatively easy to generalize (18)–(21) for the healing layer. We find that

$$\widehat{S}_0 = \widehat{S}_0(\theta, t) \tag{49}$$

where

$$\frac{\partial^2 \widehat{R}_0}{\partial \xi^2} - \widehat{R}_0^3 + \widehat{R}_0\left[1 + U^2 - \left(\frac{\partial \widehat{S}_0}{\partial \theta}\right)^2 - 2\frac{\partial \widehat{S}_0}{\partial t}\right] = 0. \tag{50}$$

The relevant solution is

$$\widehat{R}_0 = g(\theta, t)\tanh(g(\theta, t)\xi/\sqrt{2}) \tag{51}$$

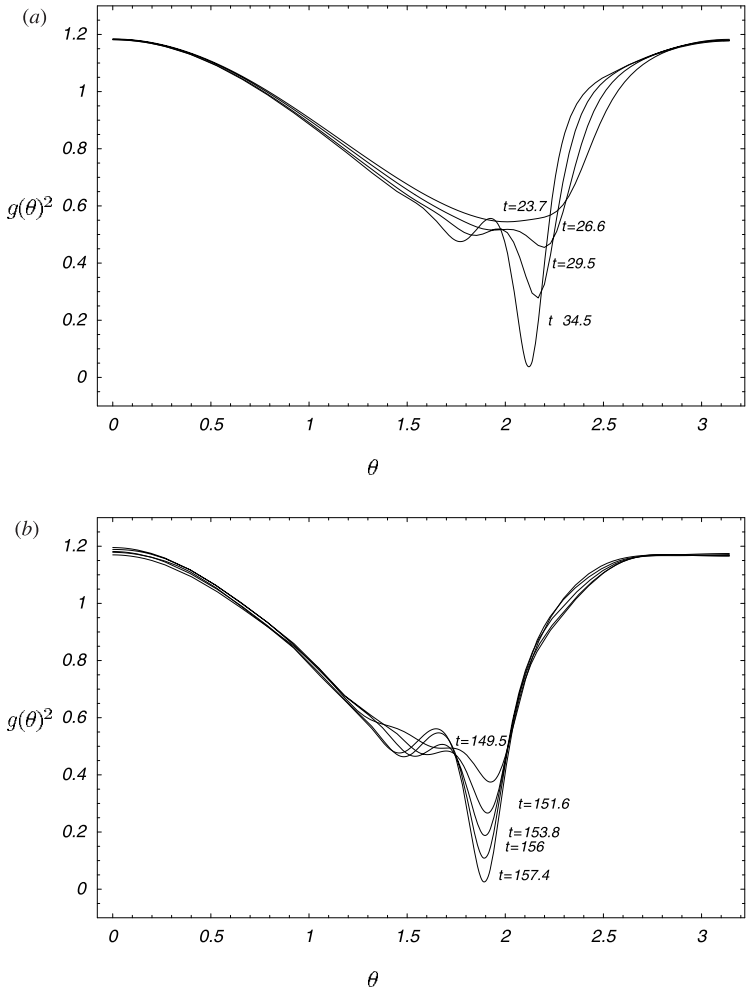

Figure 2. Time evolution of $g(\theta)^2$ defined in (52) for the flow around a sphere of radius 10 before the nucleation of the first (*a*) and the second (*b*) vortex rings; $U = 0.42$, θ in radians.

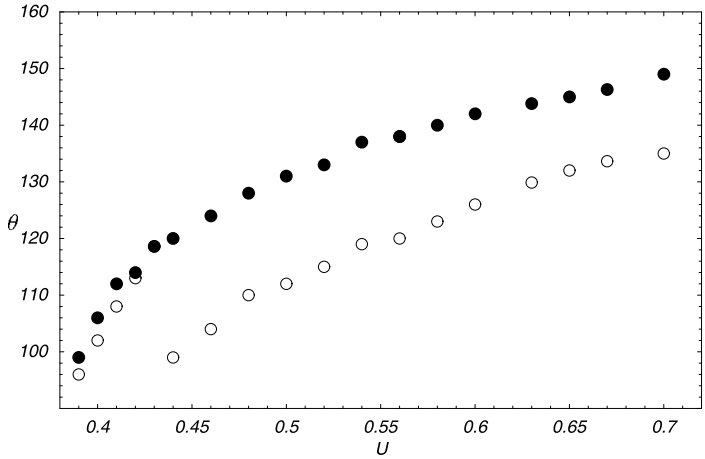

Figure 3. The values of θ at which the first two vortex rings nucleate from the surface of the ion, as a function of the velocity, U, of the ion, when $\epsilon = 0.1$. The first angle of nucleation, θ_{c_1} (full circles), increases with U. The flow velocity on the surface of the ion is reduced by the first vortex ring, and the next nucleation therefore takes place at a smaller value, θ_{c_2} (circles), of θ. The θ_{c_2} curve has two continuous branches (see text).

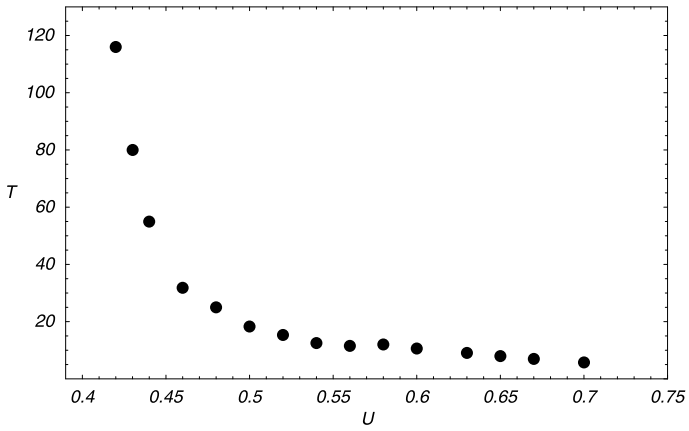

Figure 4. The time interval, T, between the nucleations of the first and second rings as a function of U for $\epsilon = 0.1$.

where now

$$g(\theta, t) = \sqrt{\left[1 + U^2 - \left(\frac{\partial \widehat{S}_0}{\partial \theta}\right)^2 - 2\frac{\partial \widehat{S}_0}{\partial t}\right]}. \tag{52}$$

The $\partial \widehat{S}_0/\partial t$ term in (52) is highly significant: as $g(\theta, t)$ approaches 0, the thickness of the healing layer tends to ∞ and the assumptions we made in our asymptotic expansions break down. Our numerical integrations indicate that the nucleation of a vortex ring occurs near latitude θ_c after time t_c, when

$$g(\theta_c, t_c) = 0 \qquad \frac{\partial g}{\partial \theta}(\theta_c, t_c) = 0. \tag{53}$$

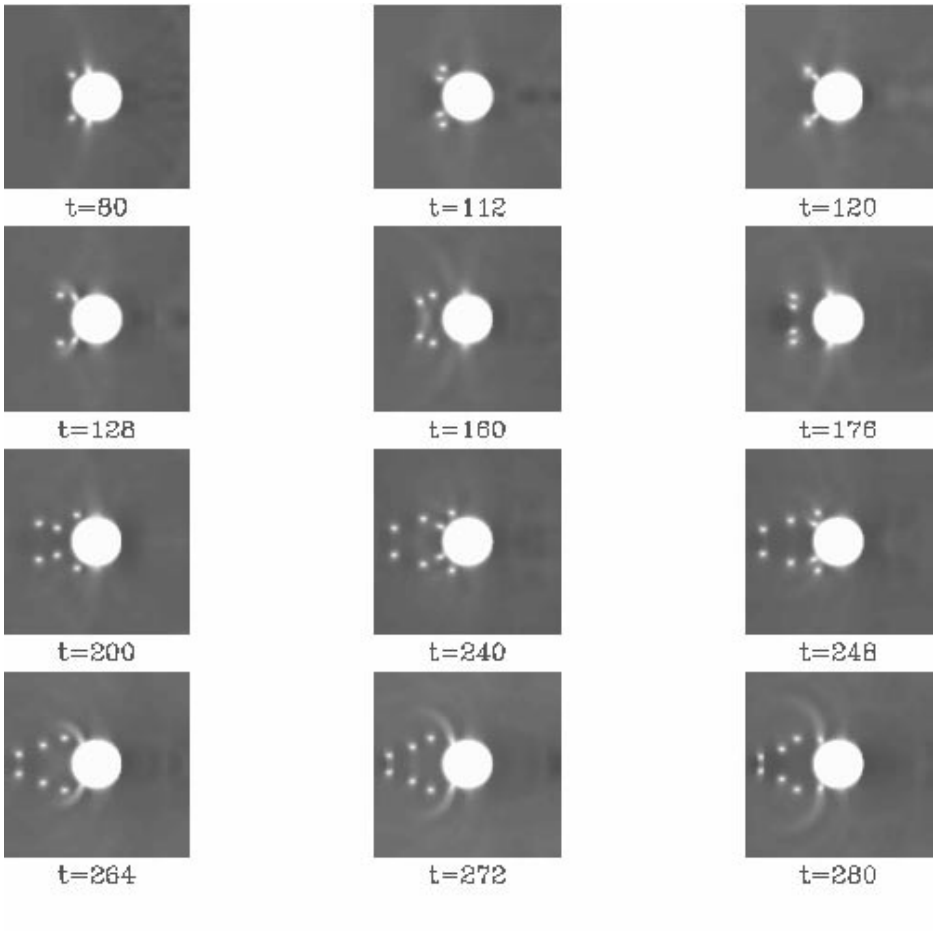

Figure 5. The density plot in a cross section of the solution of (48) for the flow around a sphere of radius 10 moving to the right with velocity 0.47. The dynamics of the turbulent wake is shown through time snapshots. Initially a vortex ring is born at $\theta_c = 124^\circ$; shortly afterwards a second ring of larger radius is nucleated at $\theta_c = 107.5^\circ$. The close proximity of these two vortex rings allows them to interact with each other and with the sphere. As these two vortices drift downstream a third vortex ring is born at $t = 176$. As a result of interactions the radius of one of the rings decreases, so that it overtakes the sphere, striking it at $t = 248$.

Thus, the nucleation of a vortex ring represents a breakdown of the healing layer. This may be traced to the growth in importance of the first term in (8) at θ_c and the concomitant decrease in significance of the final, quantum pressure. This decrease implies that, at nucleation, $\partial R/\partial \xi$ at θ_c is no larger than ∇R in the mainstream, i.e. the mainstream and healing layer have become temporarily connected. This provides the channel through which the vortex escapes from the ion. It may be noted that the breakdown ($g = 0$) of the healing layer on the supercritical ion is not directly linked to the criterion ($|\boldsymbol{v}| = c$) used to determine the critical state for the steady subcritical solutions. This explains why $\theta_c > \frac{1}{2}\pi$, even though the maximum u_θ on the sphere still occurs on the equatorial plane ($\theta = \frac{1}{2}\pi$).

As it is impractical to extend the theory of section 3 for the mainstream to the time-dependent case, and then to determine $\widehat{S}_0$ and g by matching to the healing layer, we must

determine $\widehat{S}_0$ and g from the numerical results for small ϵ. Figure 2 shows how g evolves when $\epsilon = 0.1$ and when the velocity of the ion is 0.42. The first vortex begins to form when g becomes zero at $\theta_c \approx 120^\circ$ at $t_c \approx 35$ (see figure 2(*a*)), where a second minimum in g can also be seen on the $t = 34.5$ curve near $\theta_c \approx 110^\circ$. This second minimum develops, becomes zero, and then the next vortex is nucleated (see figure 2(*b*)). The breakdown of the healing layer is very evident in figure 2, and is responsible for the two blips seen on the sphere in figure 1(*a*) and, at different θ-locations, in figure 1(*c*). It is also clear that, as the healing layer thickens at θ_c, it provides the core of the nascent vortex. The angle θ_c at which the vortex rings are nucleated is shown in figure 3 as a function of U; θ_{c_1} refers to the first vortex ring and θ_{c_2} to the second one. For $U < 0.435$, the frequency of nucleation is so low that the second ring is formed at a time when the first ring has moved so far downstream that it has only a small effect on the nucleation process; θ_{c_2} is therefore only slightly less than θ_{c_1}. As U increases, the frequency of nucleation increases, and the first ring is near enough to the ion to be influential when the second ring forms. In fact, as U approaches 0.435 the two minima of $g(\theta)$ become zero almost simultaneously, so that the second ring can be formed almost equally easily at two different locations on the sphere. When $U > 0.435$, the second minimum of $g(\theta)$ takes over from the first one, and the difference between θ_{c_1} and θ_{c_2} becomes substantial. Figure 4 supports this argument by showing how the time that elapses between the emission of the first and the second rings initially decreases rapidly with increasing U.

As the velocity of the ion increases the average frequency of nucleation of vortex rings also increases and the closer proximity of the vortex rings to each other and to the ion enhances their interaction with one another and with the ion. The result can be remarkable (figure 5): a ring can lose momentum and gain speed, causing it to overtake the ion, strike it, enlarge itself and again fall behind the ion.

6. Conclusions

We have used the Bose condensate model of superfluid helium to clarify the process through which a moving ion generates vortices if its velocity, v, exceeds a certain critical value, v_c, of the same order as the Landau critical velocity (which for the condensate, which has no roton minimum on its dispersion curve, is the speed of sound, c). To some extent, v_c depends on ϵ, the ratio of the healing length to the sphere radius. We have determined v_c analytically to first order in ϵ by equating to c the flow velocity at the equator of the ion. This does not mean, however, that the vortex ring is emitted from the equator when $v > v_c$, as was supposed by Strayer *et al* (1971), Muirhead *et al* (1984) and Frisch *et al* (1992). This was demonstrated through direct numerical simulations for small but finite ϵ. We have shown, through asymptotic analysis, that the vortex rings emerge from singularities that develop irregularly in the healing layer at some particular latitudes θ_c. We have found that θ_c increases with v, i.e. the point of detachment moves towards the rear stagnation point ($\theta = \pi$).

The development of the singularity is intimately linked to the time dependence of the mainstream supercritical flow, which fluctuates as the vortices move downstream to join the train of rings following the ion. We have not analysed what happens the first time that a vortex ring is created, but we surmise that in this case the singularity develops as the result of the instability of the mainstream flow. Thereafter, time dependence is ensured through the ring (and later rings) trailing behind the ion.

The breakdown of the healing layer is the analogue for the superfluid of boundary-layer separation in high-Reynolds-number viscous flows, and this explains the choice of subtitle for our paper.

Acknowledgment

This work was supported by the NSF grant DMS-9803480.

References

Berloff N G 1999 *J. Low Temp. Phys.* **116** 359–80
Berloff N G and Roberts P H 1999 *J. Phys. A: Math. Gen.* **32** 5611–25
Dalfovo F, Giorgini S, Pitaevslii L P and Strignari S 1999 *Rev. Mod. Phys.* **71** 463–512
Donnelly R J 1991 *Quantized Vortices in Helium II* (Cambridge: Cambridge University Press)
Frisch T, Pomeau Y and Rica S 1992 *Phys. Rev. Lett.* **69** 1644–8
Ginzburg V L and Pitaevskii L P 1958 *Zh. Eksp. Teor. Fiz.* **34** 1240–65
Grant J 1971 *J. Phys. A: Math. Gen.* **4** 695–716
Grant J and Roberts P H 1974 *J. Phys. A: Math. Gen.* **7** 260–79
Gross E P 1963 *J. Math. Phys.* **4** 195–208
Jones C A, Putterman S and Roberts P H 1986 *J. Phys. A: Math. Gen.* **19** 2991–3011
Jones C A and Roberts P H 1982 *J. Phys. A: Math. Gen.* **15** 2599–619
Muirhead C M, Vinen W F and Donnelly R J 1984 *Phil. Trans. R. Soc.* A **311** 433–67
Rayfield G W and Reif F 1964 *Phys. Rev.* A **136** 1194–208
Raymond W H and Kuo H L 1984 *Q. J. R. Met. Soc.* **110** 535–51
Roberts P H and Grant J 1971 *J. Phys. A: Math. Gen.* **4** 55–72
Strayer D M, Donnelly R J and Roberts P H 1971 *Phys. Rev. Lett.* **26** 165–9
Winiecki T, McCann J F and Adams C S 1999 *Phys. Rev. Lett.* **82** 5186–9